ASEE AMERICAN SOCIETY FOR ENGINEERING EDUCATION

Paper ID #35358

Compressive Mechanical Properties of Three-Dimensional (3D) Printed Thermoplastics

Dr. Raymond K.F. Lam, Queensborough Community College, City University of New York

Assistant professor of Engineering Technology Department of Queensborough Community College, City University of New York in Bayside, New York. He holds a Doctor of Science degree in Materials Science & Engineering from Massachusetts Institute of Technology, and a Master of Science degree and a Bachelor of Science degree in Mechanical Engineering from University of Hawaii at Manoa. Email: rlam@qcc.cuny.edu

Compressive Mechanical Properties of Three-Dimensional (3D) Printed Thermoplastics

Raymond K.F. Lam, Michael Orozco, Erick Mendieta, Bernard Hunter, and Joseph Seiter

Queensborough Community College, The City University of New York, New York, U.S.A.

---

1. Introduction

Impact and adoption rate of 3-dimensional (3D) printing in manufacturing will increase dramatically over the next few years. The market for 3D printing technology itself is expected to grow to $5.2 billion by 2020 [1]. One example is General Electric (GE)'s decision to deploy 3D printers to manufacture nozzles for its LEAP engines. GE Aviation projects have printed more than 30,000 fuel nozzle tips in 2018 [2] and GE expects to print more than 100,000 additive parts by 2020 [3]. Engineering components printed by 3-dimensional printers are employed as mechanical structures in an assembly. In order for the printed components to be useful for engineering applications, mechanical properties of printed parts must be known for structural design. The properties provide answers to the strength of the material, the types of stresses a component can endure before failure, and the size of a component based on the loads it experiences. 3D printed materials have recently been studied for their mechanical properties [4, 5, 6]. This study was undertaken to further understand the compressive mechanical properties of thermoplastic materials printed by 3D printers and provide the fundamental mechanical compression data of thermoplastic for structural design by students. This project also provided training in mechanical engineering research to two students in addition to their regular coursework in Mechanical Engineering Technology.

2. Experiment

Acrylonitrile butadiene styrene (ABS), a common type of thermoplastic material for three-dimensional (3D) printing, was the material used in the construction of the specimens for compression testing. The material was printed by three 3D printers including Stratasys Fortus 450mc Printer (Figure 1), Stratasys Mojo Printer (Figure 2), and Stratasys uPrint SE Plus Printer (Figure 3). The printers employed the 3D deposition technology of fused deposition modeling (FDM) process. Fused deposition modeling process extrudes molten thermoplastic material through a nozzle, deposits the molten material as a cylindrical layer on a planar substrate initially or on a previously deposited thermoplastic layer at subsequent depositions, and solidified in situ. The process repeated itself until a three-dimensional structure was formed. The manufacturing process is known as 3D printing or additive manufacturing.

Specimens of cylindrical shape were printed at nominal dimensions of 13 mm in diameter and 20 mm in height. They were printed at a combination of raster angles of 0 degree, 45 degrees, and 90 degrees, and orientations of flat and upright. Figure 4 shows the print orientations of each set of specimens printed by a printer. Two specimens were each printed at

flat-0 degree, flat-45 degrees, flat-90 degrees, and upright print orientations. The specimens were identified as “0”, “45”, “90”, and “UP” on the top surface to represent printing orientation of flat at 0 degree, flat at 45 degrees, flat at 90 degrees, and upright, respectively. Two specimens were printed at each combination of raster angle and orientation for testing repeatability. All eight specimens were printed at the same time in a run. Each set of specimens was further printed in both solid and sparse internal structure. The solid internal structure was formed by direct deposition of one layer on top of another layer, while the sparse internal structure was created by deposition of a porous interior network structure enclosed by an exterior envelope of solid layer. A specimen printed by a 3D printer before compression test is showed in Figure 5. Specimen identifications with print orientation and sample number are listed in Table 1.

Table 1: Specimen Identification

Specimen Identification	Print Orientation	Sample Number
0-1	Flat-0 degree	1
0-2	Flat-0 degree	2
45-1	Flat-45 degrees	1
45-2	Flat-45 degrees	2
90-1	Flat-90 degrees	1
90-2	Flat-90 degrees	2
UP-1	Upright	1
UP-2	Upright	2

A universal testing machine, PASCO model ME-8244 Comprehensive Materials Testing System with 7100 Newton capacity (Figure 6), was employed to measured mechanical properties of thermoplastic. A specimen was mounted on the machine and subjected to a compression test. The specimen was pressed by a compression force until failure or ultimate compressive strength was attained. Applied force and specimen length were continuously measured and converted respectively to engineering stress and engineering strain during the test. The data were recorded at 0.2 second intervals. Typical compression test graph of solid structure and sparse structure are showed in Figure 7 and 8, respectively. A smooth curve was recorded in the stress-strain curve of solid specimens. A jagged stress-strain curve was however found in sparse specimens. The jagged appearance was caused by the low resolution in sampling at 0.2-second intervals and the crumbling of the internal network system of the sparse structure under compression.

Figure 1. Stratasys Fortus 450mc Printer

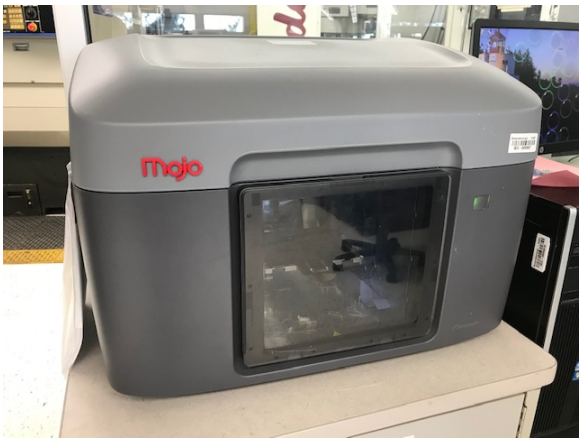

Figure 2. Stratasys Mojo Printer


Figure 3. Stratasys uPrint SE Plus Printer

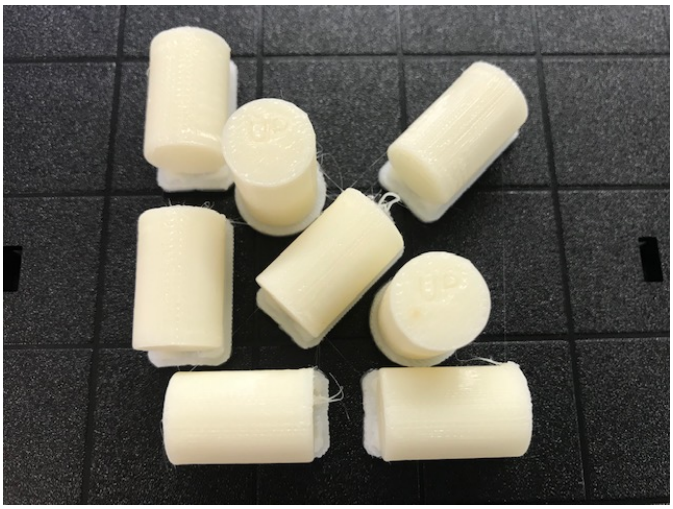

Figure 4. Orientations of Specimens at 3D Printing

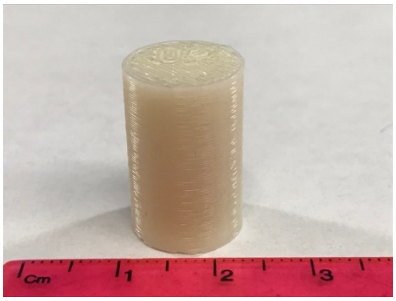

Figure 5. Specimen in Sparse Structure printed by Fortus Before Compression Test

Figure 6. PASCO ME-8244 Comprehensive Materials Testing System

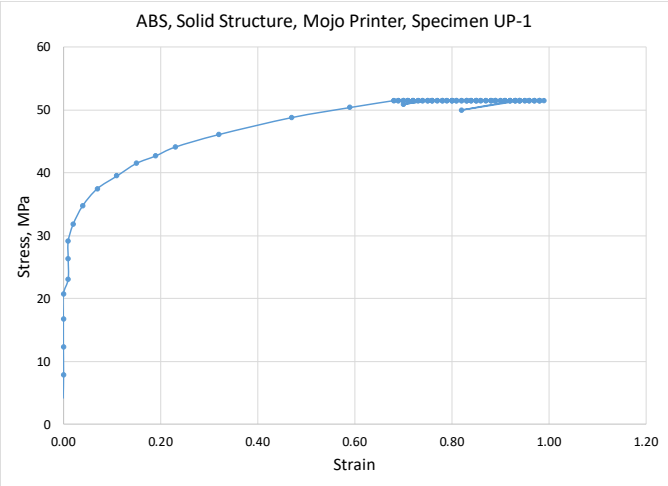

Figure 7. Compression Test Data of ABS, Solid Structure, Mojo Printer, Specimen UP-1

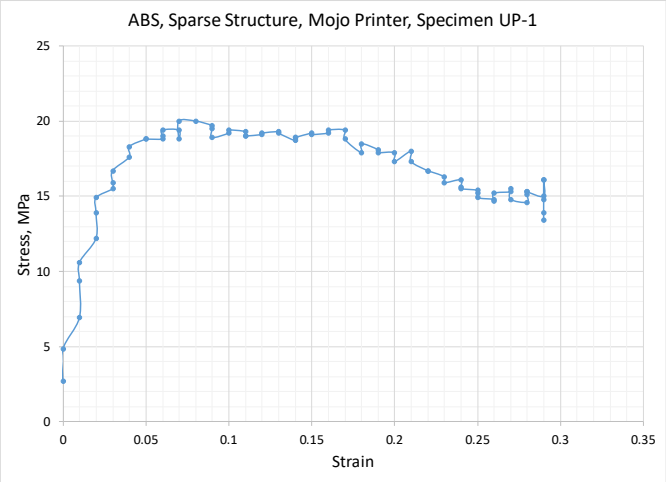

Figure 8. Compression Test Data of ABS, Sparse Structure, Mojo Printer, Specimen UP-1

3. Results and Discussion

3.1 Stress and Strain of Solid and Sparse Specimens

ABS thermoplastic in solid structure was stronger than that in sparse structure in compression. Stress experimental data as a function of time of solid and sparse specimens at flat-45º printed by Mojo printer are compared in Figure 9, while strain of the two structures at flat-45º printed by Mojo printer are compared in Figure 10. The ultimate compression strengths and strains of solid structures were more than double of those of sparse structures.

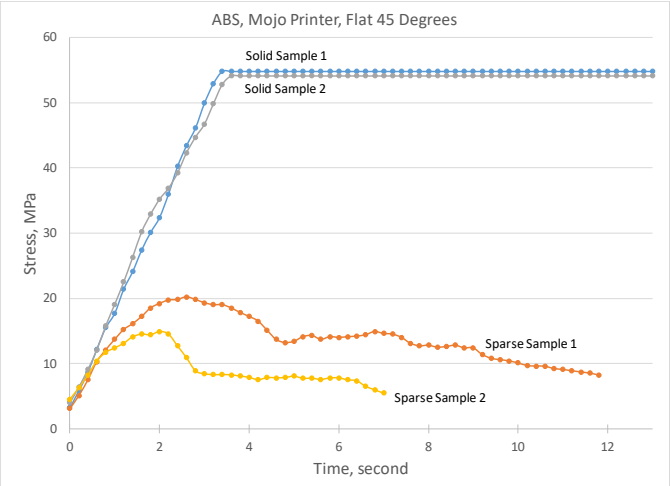

Figure 9. Comparison of Stress of Solid and Sparse Structure of Flat 45 Degrees by Mojo Printer

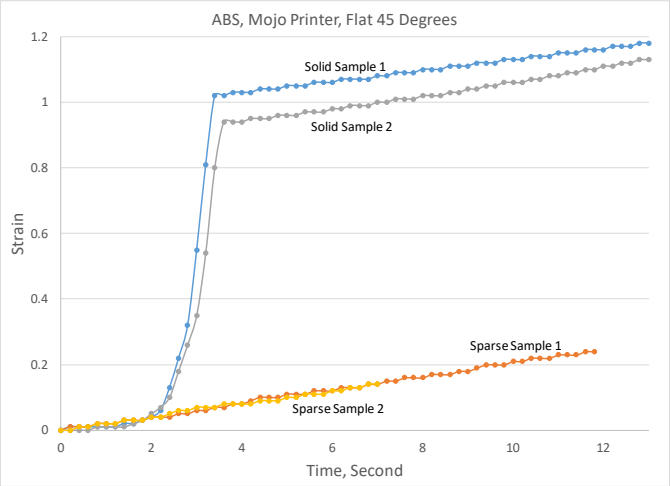

Figure 10. Comparison of Strain of Solid and Sparse Structure of Flat 45 Degrees by Mojo Printer

3.2 Ultimate Compressive Strength

Ultimate compressive strength of ABS thermoplastic, which is the highest stress on the stress-strain curve, is depicted in Figure 11. Ultimate compressive strengths of solid structure printed by Fortus, Mojo, and uPrint, ranged from 49.6 MPa to 55.3 MPa, 51.5 MPa to 55.3 MPa, and 49.9 MPa to 55.3 MPa, respectively. Ultimate compressive strengths of sparse structure printed by Fortus, Mojo, and uPrint varied from 22.4 MPa to 29.5 MPa, 14.9 to 20.3 MPa, and 18.6 MPa to 22.4 MPa, respectively. Overall, ultimate compressive strengths of solid structure ranged from 49.6 MPa to 55.3 MPa, and those of sparse structure varied from 14.9 MPa to 29.5 MPa. Ultimate compressive strength of solid structure was approximately twice that of sparse structure.

In view of orientation effect, distinctive pattern in ultimate compressive strength among print orientations of flat-0°, flat-45°, flat-90°, and upright was not observed in Figure 11. Ultimate compressive strength remained relative constant among all print orientations in the same internal structure printed by a particular printer.

In comparison of the data among specimens produced by various printers, ultimate compressive strengths of solid structure printed by Mojo were slightly higher than those printed by the other two printers. Maximum variations in ultimate compressive strength of solid structure among printers ranged from 0.1 MPa to 5.7 MPa (Figure 12). The variations were relatively insignificant. Effect of printer on ultimate compressive strength of solid structure was therefore not found. Ultimate compressive strengths of sparse structure demonstrated larger variations among printers (Figure 11). The ultimate compressive strengths of sparse structure printed by Fortus printer were predominately higher than those printed by the other two printers with values exceeding from 3.5 MPa to 10.1 MPa (Figure 12). The sparse structure produced by Fortus printer was therefore stronger than those manufactured by Mojo and uPrint.

Specific ultimate compressive strength, which is the strength per unit density, is depicted in Figure 13. Density of solid structure by Fortus, sparse structure by Fortus, solid structure by Mojo, sparse structure by Mojo, solid structure by uPrint, and sparse structure by uPrint were 0.982 g/cm^3, 0.598 g/cm^3, 1.06 g/cm^3, 0.694 g/cm^3, 1.01 g/cm^3, and 0.598 g/cm^3, respectively. The specific compressive strengths of solid structures among all printers were comparable. In view of the specific compressive strength of sparse structures, samples printed by Fortus were consistently stronger than those by uPrint and, in turn, samples printer by uPrint were stronger than those printed by Mojo.

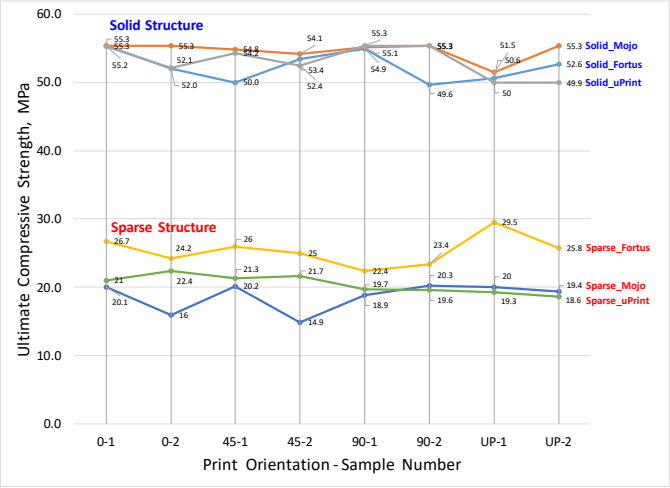

Figure 11. Ultimate Compressive Strength of ABS Thermoplastic

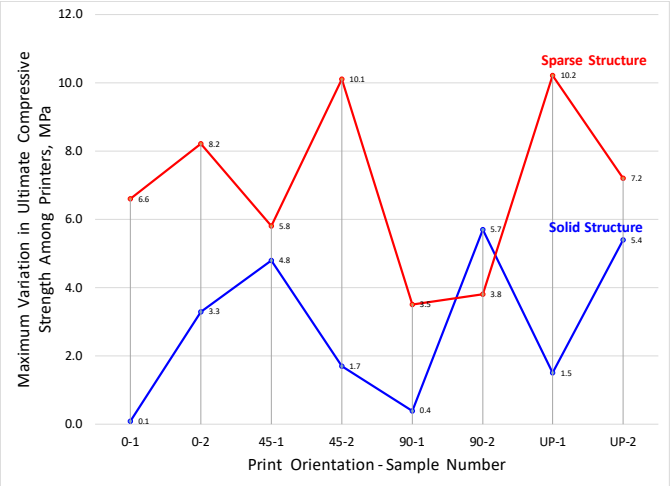

Figure 12. Maximum Variation in Ultimate Compressive Strength among Printers

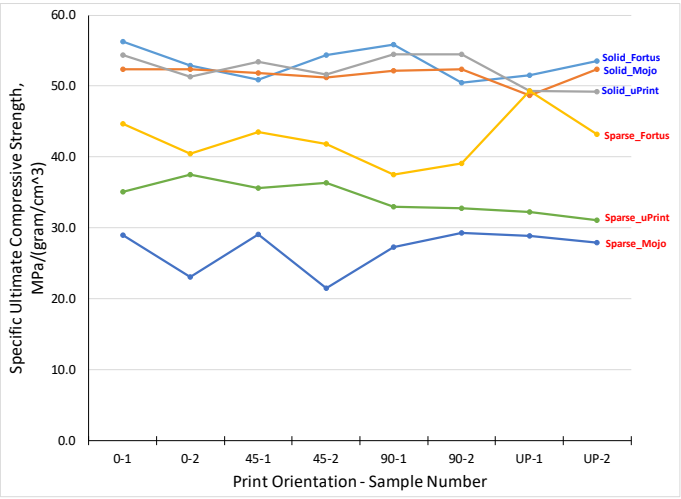

Figure 13. Specific Ultimate Compressive Strength of ABS Thermoplastic

3.3 Ultimate Compressive Strain

Figure 14 presents ultimate compressive strain that is the strain at which ultimate compressive strength is reached. Ultimate compressive strains of solid structure varied from 0.60 to 1.2; while those of sparse structure ranged from 0.04 to 0.15. ABS thermoplastic could therefore sustain minor degrees of deformation before the highest stress level was attained. Ultimate compressive strains of solid structures were significantly higher than those of sparse structures. Sparse structures were weak and they can be easily compressed with a reduced amount of deformation to reach their ultimate compressive strengths.

Effect of print orientation on ultimate compressive strain was not apparent as showed in Figure 14. Data of solid structures were so scattered that effect of print orientation in solid structures on ultimate compressive strain was inconclusive. Ultimate compressive strains of upright print orientation in sparse structure exhibited slightly higher ultimate compressive strains

than those of flat print orientations. The ultimate compressive strains of upright print orientation ranged from 0.06 to 0.15, while those of the three flat print orientations varied from 0.04 to 0.07. This implied that the sparse structure in upright print orientation demonstrated a higher degree of compression deformation than those of flat print orientations, exceeding by approximately 3 times.

Printer effect on ultimate compressive strain was not found. In reference to the ultimate compressive strain in Figure 14, sparse structure produced by Fortus printer exhibited higher compressive strengths in all print orientations and generally higher compressive strains in the upright orientation in comparison with sparse structures printed by Mojo and uPrint.

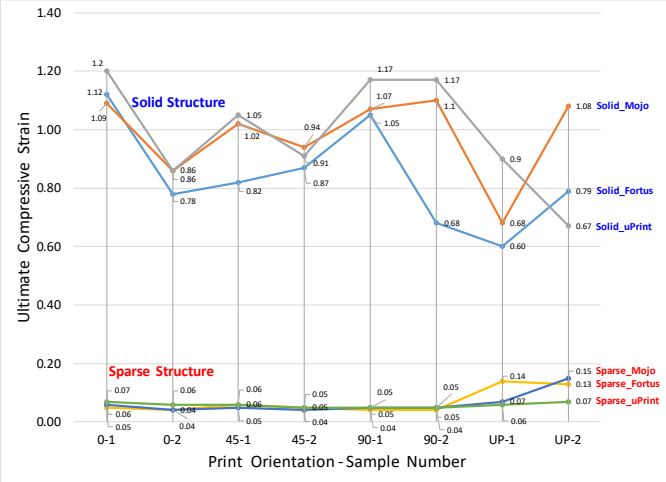

Figure 14. Ultimate Compressive Strain of ABS Thermoplastic

3.4 Modulus of Elasticity

Figure 15 shows modulus of elasticity that is the slope of the stress-strain curve of elastic deformation. The slope was determined by using the data points in the linear section of the stress-strain curve. The modulus of elasticity of ABS overall varied from 305 MPa to 1046 MPa. No distinct pattern of change in modulus of elasticity in reference to print orientation was found. Effect of print orientation on modulus of elasticity was therefore not observed.

Modulus of elasticity of solid structures printed by Fortus, Mojo, and uPrint ranged from 305 MPa to 725 MPa, 555 MPa to 1046 MPa, and 585 MPa to 776 MPa, respectively. Modulus of elasticity of sparse structures printed by Fortus, Mojo, and uPrint varied from 524 MPa to 685 MPa, 306 MPa to 484 MPa, and 337 MPa to 531 MPa, respectively. Values of modulus of elasticity of solid structures were generally greater than those of sparse structures. Greater stress was thus required to compress solid structures to the same amount of strain than that to sparse structures in elastic deformation. Solid structures are therefore stronger than sparse structures.

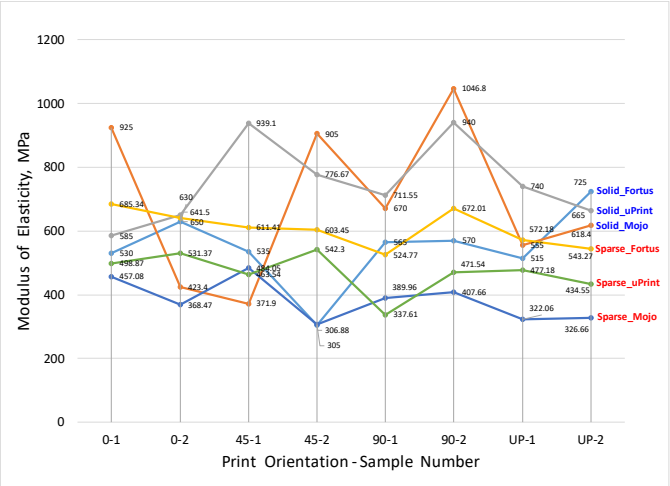

Figure 15. Modulus of Elasticity of ABS Thermoplastic

3.5 Yield Strength

Figure 16 depicts yield strength that is the transition point from elastic deformation to plastic deformation. The yield strength is the endpoint of linear part of the stress-strain curve. The 0.2% offset rule was not employed. Yield strength of solid structures varied from 33.6 MPa to 39.3 MPa, while yield strength of sparse structure ranged from 14.5 MPa to 27.9 MPa. Yield strengths of solid structures were approximately two times those of sparse structures.

Yield strength of each orientation printed by a printer were found to have similar values. Effect of print orientation on yield strength was therefore not observed.

Yield strength of solid structures printed by Fortus, Mojo, and uPrint was measured to be 33.6 MPa to 37.2 MPa, 34.8 MPa to 36.9 MPa, and 34.1 MPa to 39.3 MPa, respectively. Yield strength of sparse structures printed by Fortus, Mojo, and uPrint varied from 22.1 MPa to 27.9 MPa, 14.5 MPa to 19.8 MPa, and 18.1 MPa to 22.1 MPa, respectively.

Yield strengths of solid structures printed by the three printers were similar to each other. Maximum variations in yield strength ranged from 0.6 MPa to 2.7 MPa (Figure 17). These variations were insignificant in specimens produced by the three printers.

Yield strengths of sparse structure printed by Fortus exhibited values higher than those of sparse structures printed by Mojo and uPrint. The yield strength values of Fortus exceeded those of the two other printer by 3.1 MPa to 10.1 MPa (Figure 17). The sparse structure manufactured by Fortus was thus stronger than those sparse structures produced by Mojo and uPrint.

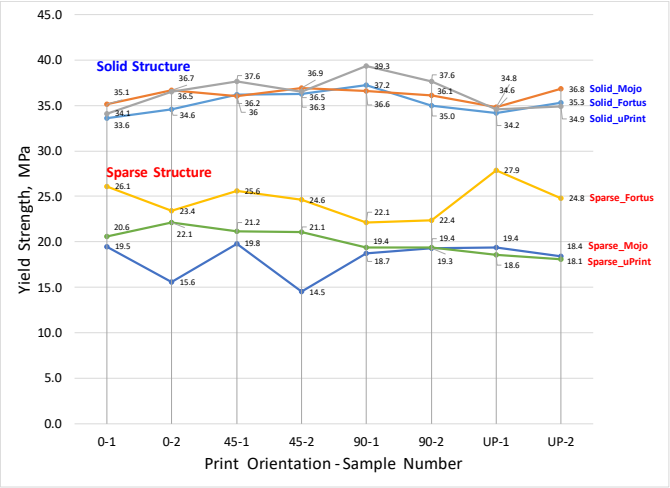

Figure 16. Yield Strength of ABS Thermoplastic

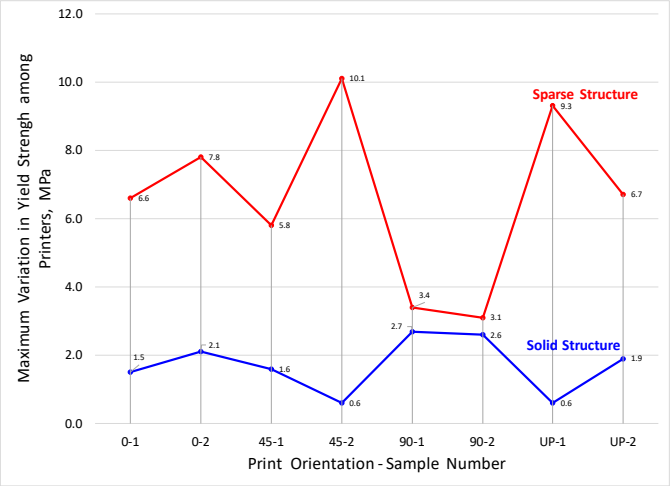

Figure 17. Maximum Variation in Yield Strength among Printers

3.6 Yield Strain

Figure 18 depicts yield strain that is the strain when yield strength occurs. Yield strain of ABS thermoplastic varied from 0.03 to 0.12. ABS could be deformed at a small degree before the deformation was transformed from elastic mode to plastic mode. Effects of print orientation and printer on yield strain were not observed.

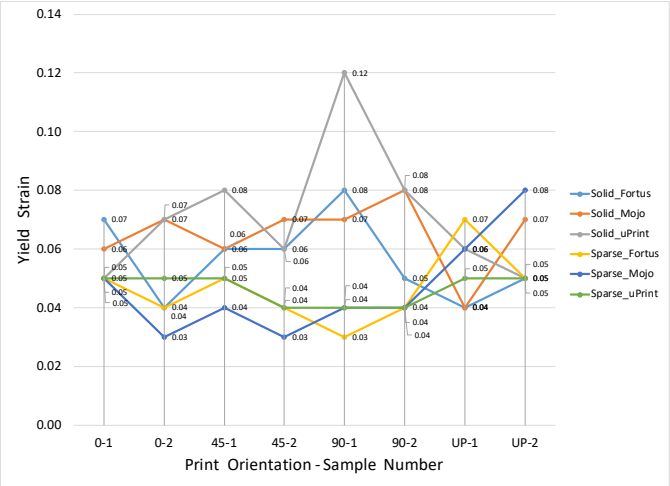

Figure 18. Yield Strain of ABS Thermoplastic

3.7 Failure Mode

Solid structures at flat-90° print orientation and upright orientation printed by Mojo after compression test are respectively showed in Figure 19 and 21. Compression force was sustained by the entire solid body of the specimen. Compressive plastic deformation transformed an initial cylindrical shape into a barrel shape as the highest deformation occurred at the middle portion of the cylinder.

Sparse structures printed by Mojo at flat-90° print orientation after compression test is depicted in Figure 20. Exterior layer that enclosed the sparse structure was the load bearing component of the structure. The exterior layer sustained compression force until the exterior layer failed by buckling, at the same time the interior network of porous structure collapsed under the force. The exterior layer was formed by deposition of layers in the direction parallel to the longitudinal axis of the specimen cylinder when the specimen was printed flat. As the exterior layer buckled, the layer folded perpendicular to the direction of 3D layer deposition and away from the centerline of the cylinder. Meanwhile, the interior porous structure was reduced in size in longitudinal direction. The folding of the exterior layer at buckling extended the outer diameter of the layer and contributed to the large increase in lateral strain. This type of exterior layer buckling failure was also observed in the other two print orientations of flat-0° and flat-45°.

Due to the fact that higher values in specific ultimate compressive strength (Figure 13) of the sparse structure printed by Fortus in comparison with the sparse structures printed by Mojo and uPrint, the exterior layer produced by Fortus was stronger than those produced by the other two printers. The exterior layer printed by Fortus failed by buckling in a catastrophic manner and the layers separated and folded extensively (Figure 23).

Figure 22 depicts specimens with sparse structures at upright orientation printed by Mojo after compression test. Specimens in the upright orientation was produced by 3D deposition of layers perpendicular to the longitudinal axis of specimen cylinder. The exterior solid layer in sparse structure was also the load bearing component in compression. As the exterior layer

buckled and the interior porous layer collapsed, the exterior layer folded in the same direction of 3D layer deposition. The buckling occurred along the joint between deposition layers, the exterior layer were easily folded with little extension outside its outer diameter. The lateral strain of sparse structure in upright print orientation was therefore not as high as those at flat-0°, flat-45°, and flat-90°.

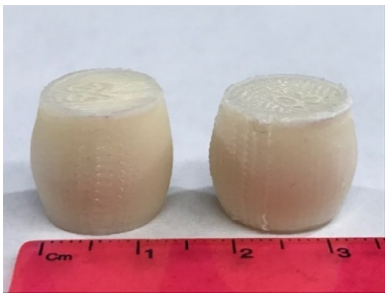

Figure 19. ABS Specimens of Solid Structure Printed by Mojo at flat-90° Print Orientation After Compression Test.

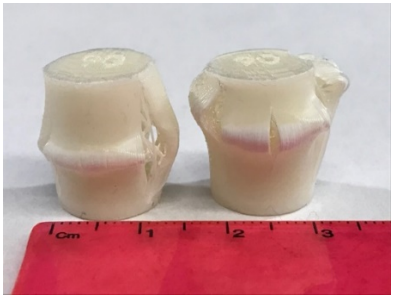

Figure 20. ABS Specimens of Sparse Structure Printed by Mojo at flat-90° Print Orientation After Compression Test.

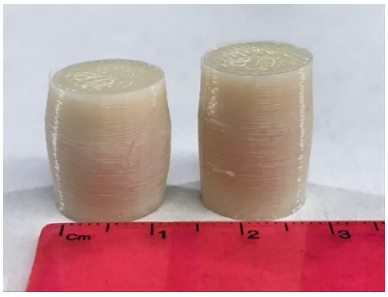

Figure 21. ABS Specimens of Solid Structure Printed by Mojo at Upright Orientation After Compression Test.

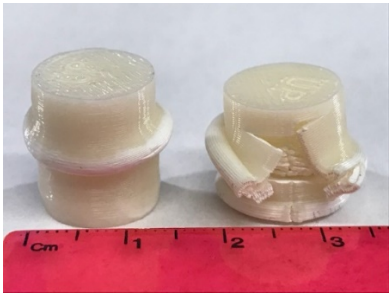

Figure 22. ABS Specimens of Sparse Structure Printed by Mojo at Upright Orientation After Compression Test.

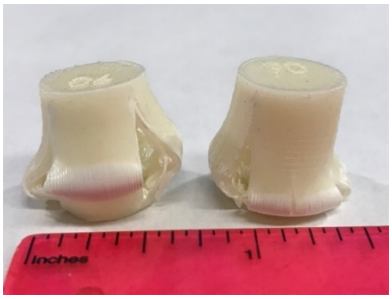

Figure 23. ABS Specimens of Sparse Structure Printed by Fortus at flat-90° Print Orientation After Compression Test.

4. Conclusion

Ultimate compressive strength, ultimate compressive strain, modulus of elasticity, yield strength, yield strain, Poisson's ratio, and failure mode of acrylonitrile butadiene styrene (ABS) thermoplastic printed by Fortus, Mojo, and uPrint printers at print orientations of flat-0°, flat-45°, flat-90°, and upright with solid and sparse structures under compression were examined in this study.

Solid structures were significantly stronger than sparse structures. Ultimate compressive strength and yield strength of solid structures were larger than those of sparse structure by approximately two times. Solid structures were more difficult to deform in the elastic region than sparse structures, as the moduli of elasticity of solid structures were generally higher than those of sparse structures.

ABS thermoplastic both in solid structure and sparse structure exhibited very limited elastic deformation before transition from elastic to plastic deformation. Yield strain of ABS thermoplastic varied from 0.03 to 0.12. Plastic deformation was therefore limited before ultimate compressive strength occurred. Ultimate compressive strains of solid structures varied from 0.60 to 1.2; while those of sparse structures ranged from 0.04 to 0.15. Plastic deformation at ultimate compressive strength of solid structure was 8 to 15 times that of sparse structure.

Effects of flat print orientations on mechanical properties of ultimate compressive strength, ultimate compressive strain, yield strength, yield strain, and modulus of elasticity were not observed.

Solid structures at all print orientations failed in the classical way by forming a barrel shape from a cylindrical shape, as high degrees of deformation occurred at the mid-section of the cylinder. Exterior layer of sparse structure was the main load bearing component in compression. Buckling of the exterior layer in sparse structure was the failure mode as the interior porous network structure collapsed under compression. The buckling in sparse specimens with flat-0°, flat-45°, and flat-90° print orientations occurred perpendicular to the 3D printing deposition direction, while the buckling in sparse specimens with upright print orientation occurred parallel to the 3D printing deposition direction. The buckling in flat oriented specimens in sparse structure was more extensive than that of upright oriented specimens.

Based on the data of ultimate compressive strength and yield strength, sparse structures produced by Fortus demonstrated higher strength and greater degree of brittle buckling with catastrophic failure than those of sparse structures produced by Mojo and uPrint.

The specific compressive strengths of solid structures among all printers were comparable. In view of the specific compressive strength of sparse structures, samples of sparse structures printed by Fortus were consistently stronger than those by uPrint and, in turn, those samples printed by uPrint were stronger than those by Mojo.

5. Acknowledgement

This study and training of two mechanical engineering technology students in research are supported by Professional Staff Congress/The City University of New York (PSC/CUNY) Research Award #62222-00-50. The supports by the Engineering Technology Department of Queensborough Community College in Bayside, New York is greatly appreciated. The authors are grateful to Professor Hamid Namdar (department chair), Professor Stuart Asser (former department chair), and Mr. Jerry Sitbon (chief college laboratory technician) for their supports, encouragement, and guidance.

6. References

[1] B. Thompson, "How 3D Printing Will Impact The Manufacturing Industry," *Manufacturing Business Technology*, Jan., 2016.

[2] B. Jackson, "GE Aviation Celebration 30,000th 3D Printed Fuel Nozzle", 3D Printing Industry, Oct. 2018.

[3] N. Sankar, K. Natarayan, G. Iyer, A. Kalathil, "Printing the Future: From Prototype to Production," *Cognizant 20-20 Insights*, pp. 1-8, Nov., 2015.

[4] T. Letcher, M. Waytashek, "Material Property Testing of 3D-Printed Specimen in PLA on an Entry-Level 3D Printer," *ASME IMECE 2014 Proceedings*, Montreal, Canada, IMECE2014-39379, 2014.

[5] B. M. Tymrak, M. Kreiger, J. M. Pearce, "Mechanical Properties of Components Fabricated with Open-Source 3-D Printers Under Realistic Environmental Conditions," *Materials & Design*, vol. 58, pp. 242-246, 2014.

[6] B. Rankouhi, S. Javadpour, F. Delfanian, T. Letcher, "Failure Analysis and Mechanical Characterization of 3D Printed ABS With Respect to Layer Thickness and Orientation," *Journal of Failure Analysis and Prevention*, vol. 16, pp. 467-481, Jun., 2016.